# Haptic Control of the Hand Force Feedback System

G.M. Prisco, M. Ortiz, F. Barbagli, C.A. Avizzano, M. Bergamasco

PERCRO, Scuola Superiore S.Anna,
Via Carducci, 40
56127 Pisa
Italy

## ABSTRACT

The Hand Force Feedback System is an anthropomorphic haptic interface for the replication of the forces arising during grasping and fine manipulation operations. It is composed of four independent finger dorsal exoskeletons which wrap up four fingers of the human hand (the little finger is excluded). Each finger possesses three electrically actuated DOF placed in correspondence with the human finger flexion axes and a passive DOF allowing finger abduction movements.

Each exoskeleton finger has three points of attachment to the operator's finger (two for the thumb) at the middle of the phalanges. Mechanical fixtures guarantee that just a force perpendicular to the finger and in its sagittal plane is exchanged at each point of attachment. Such force component is sensed and it is actively controlled in feedback.

The present paper illustrates the design and testing of the controller for the thumb exoskeleton. First the mechanical system is analyzed and the features which influence the controller design, such as the presence of unidirectional tendon transmission, are modeled. Then haptic controllers, i.e. feedback controllers aiming at improving the performance of the device when used as haptic interface for Virtual Environments or Telemanipulation, are designed and tested experimentally.

Finally the experimental results are discussed.

**Keywords:** Haptic Interface, Hand, Tension Tendon Transmission, Virtual Environments, Force Feedback, Force Control

## 1. INTRODUCTION

Haptic interfaces for Virtual Environments are robotic systems which aim at reproducing on the operator sensations of contact between his/her body and virtual objects. Such interfaces realize a bi-directional flow of information and energy. On one side the haptic interface sends information about the operator's estimated position and velocity to the virtual environment. On the other side the haptic interface replicates the interaction forces with virtual objects on the operator.

In this paper we focus on the HFF - Hand Force Feedback, an anthropomorphic hand controller for teleoperation and Virtual Environment applications.[1] The design of a haptic interface for the human hand is a very complex matter. This is due to the fact that the possible interactions between a human hand and any object are very different one from the other, according to the purpose of such contact and the type of object involved.[2] Contacts with real objects concern the whole surface of the hand. Ideally an infinite number of actuators positioned all over the user's hand would be required. In practice a limited number of actuators and of contact points with the human finger have to be chosen.

A practical solution to this problem is to reduce the number of possible interactions between a phalange and the virtual environment to one single force, perpendicular to the finger and laying in its sagittal plane (see fig.1).

Further author information, send correspondence to:
Giuseppe Maria Prisco, e-mail: gmprisco@sssup.it
Federico Barbagli, e-mail: fed@sssup.it
Massimo Bergamasco, e-mail bergamasco@percro.sssup.it

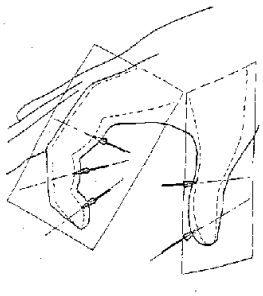

**Figure 1.** Forces replied by the HFF and the TES.

Actuators are a limiting factor for a hand haptic interface which ideally should be at the same time light, easily wearable and capable of creating a realistic feeling of a virtual environment possibly without the user realizing its presence.

One of the possible ways to overcome the limitations of state-of-the-art actuator technologies is to design making use of tendon transmission.[4,5,8] Using such a design technique, it is possible to locate the actuators away from the joint axis. This means that constraints on weight and volume of the actuators are partially relaxed and that the moving mass of the link can be reduced. This is obviously of extreme importance when designing a hand haptic interface, being the room between fingers extremely limited.

Among the wide range of possible tendon transmission designs, tension tendon transmission deserves a special consideration due to its low friction, high efficiency and backdrivability, which is a key issue for haptic interfaces. The key point of such a transmission is that tendons are routed over idle pulleys and are prevented to go slack being a minimum tension always guaranteed. Comparing such a transmission with the ones based upon tendons in shelths shows how in the former case force control capabilities are much better even though the whole mechanical system results in being much more complex. The technical choice at PERCRO in designing the HFF is to go for a tension tendon drive.

Tension tendon transmission though introduces new phenomena which have to be analyzed to properly control haptic interfaces. First of all, the presence of elastic tendons connecting the motor inertia to the link inertia determines a resonant mode at a frequency usually lower than the one associated to the structural elasticity of the links. Secondly, tension tendon drive in multi-DOF robots with serial kinematics causes a phenomenon, known as coupling between joint torque and motor torque, not present at all in robots with actuators on the joints. The torque at a joint is not determined exclusively by the actuator directly connected to it, but also by the actuators connected to the tendons passing on that joint to reach a successive link of the robot.[6]

A special type of tendon transmission is the unidirectional one, meaning that there is only one tendon from the actuator to the link to be controlled. This implies that the actuator connected to a certain link is only actively moving it in one direction. When the link moves in the other direction, being the actuator passive, return springs have to be used to make sure that the tendon's tension is kept at a minimum level.

The present paper illustrates the design and testing of a haptic controller for the thumb exoskeleton, which is a part of the HFF. Referring to fig.2 the human operator is modeled as a 1-port impedance $Z_h$. $Z_h$ is an input-output representation of a casual, possibly non linear, time-varying dynamic system and it does not imply any hypothesis on the human operator behavior. $f_h$ represents the force applied by the haptic interface on the human operator while $v_h$ is the common velocity of the point of attachment of the haptic interface to the human operator. $Z_v$ on the other side represents the virtual environment modeled as a digital system. Our purpose is to design block C, the haptic controller, to work for different conditions, i.e. when block $Z_h$ represents a human operator or an infinitely rigid environment and when block $Z_v$ is null, meaning that no virtual object is being simulated, or when it represents an elastic virtual object. $f_v$ represents the reference input for such controller while $f_h^*$ represents a measure of $f_h$ fed back through the haptic interface. In this framework haptic interfaces are seen as systems having two ports[7] through which they interact with the virtual environment and with the operator.

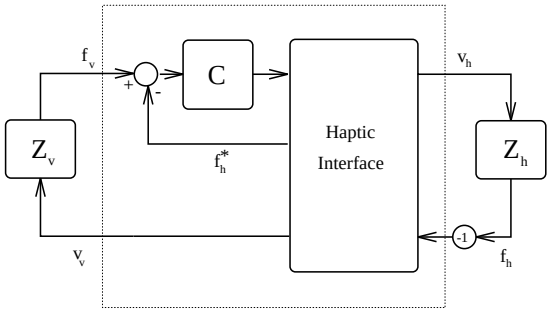


**Figure 2.** Haptic interface for virtual environments as a 2 port with a force servo.

The reminder of this paper is organized as follows. In section 3 we focus on the HFF mechanical system and the Thumb Exos System - TES. In section 4 the features which influence the controller design, such as the presence of unidirectional tension tendon transmission, are modeled. Then the design of haptic controllers, i.e. feedback controllers aiming at improving the performance of the device when used as haptic interface for Virtual Environments or Telemanipulation, is presented in section 5. Finally in section 6 the experimental results are discussed.

## 2. NOMENCLATURE

| | | | |
|---|---|---|---|
| $\tau_{m,i}$ | Electromagnetic torque for motor $i$. | $\boldsymbol{q}$ | Vector $[q_1, q_2, q_3]$. |
| $\tau_i$ | Torque at joint $i$. | $\boldsymbol{q_m}$ | Vector $[q_{m,1}, q_{m,2}, q_{m,3}]$. |
| $\tau_{dp,i}$ | Torque applied by transmission $i$ on driving pulley $i$. | $\boldsymbol{\tau}$ | Vector $[\tau_1, \tau_2, \tau_3]$. |
| $\tau_{load,i}$ | Load torque applied on rotor $i$. | $\boldsymbol{\tau_m}$ | Vector $[\tau_{m,1}, \tau_{m,2}, \tau_{m,3}]$. |
| $q_{m,i}$ | Rorot angular displacement for motor $i$. | $\boldsymbol{f}$ | Vector $[0, f_2, f_3]$. |
| $q_{dp,i}$ | Angular displacement for driving pulley $i$. | $\boldsymbol{\Phi}$ | Vector $[0, \Phi_2, \Phi_3]$. |
| $q_i$ | Angular displacement for joint $i$. | $\boldsymbol{N}$ | Decoupling matrix for tendon transmission. |
| $N_i$ | Reduction ratio for gearbox applied to motor $i$. | $\boldsymbol{J(q)}$ | Jacobian matrix for vector $\boldsymbol{q}$. |
| $N_{t,i}$ | Transmission ratio for tendon $i$. | $\boldsymbol{K}$ | Matrix diag$[0, K_2, K_3]$. |
| $J_{m,i}$ | Rotor inertia of motor $i$. | $f_c(t)$ | Control action theoretically computed for the gene |
| $J_{dp,i}$ | Inertia of driving pulley $i$. | $f(t)$ | Measured force on the generic link. |
| $J_{l,i}$ | Total inertia for driven pulley fixed wuth link $i$ and link $i$. | $f_d(t)$ | Desired force on the generic link. |
| $k_{t,i}$ | Elastic constant for tendon $i$. | $T_d$ | Derivation time for the PID derivative term. |
| $b_{t,i}$ | Viscous coefficient for tendon $i$. | $T$ | Sampling time for the controller. |
| $b_{m,i}$ | Rotor viscous coefficient for motor $i$. | $T_i$ | Integration time for the PID integrative term. |
| $r_{ii}$ | Radius of driven pulley fixed to link $i$. | $K$ | $mboxProportionalterm'sgainforthePIDcontrolli$ |
| $r_{i,j}$ | Radius of idle pulley for tendon $i$ fixed with link $j$. | $K_d$ | Derivative term's gain for the PID controlling acti |
| $r_{dp,i}$ | Radius of driving pulley $i$. | $I(k)$ | Integral term of the PID controlling action. |
| $T_{t,i}$ | Tension of tendon $i$. | $D(k)$ | Derivative term of the PID controlling action. |
| $K_i$ | Elastic coefficient for return spring $i$. | $P(k)$ | Proportional term of the PID controlling action. |

## 3. SYSTEM DESCRIPTION

The HFF[1] is composed of four exoskeletons (fig.3,a), each of which exerting forces to the phalanges of the hand's fingers (little finger excluded), that all together can be worn as a glove by the user. Each finger exoskeleton consists of four links connected by revolute joints disposed as the joints of each finger. For each joint of the finger exoskeleton, the joint axis has been designed in order to approximate the instantaneous position of the human flexion-extension axis during operation. At the metacarpo-phalangeal joint a passive abduction-adduction movement has been also integrated.

More specifically we will focus our attention on the TES (fig.3,b). The TES is slightly different from the other finger exoskeletons. In particular, from a construction point of view, the cantilever supporting the three motors of the thumb assumes a completely different aspect with respect to the ones of the other fingers. Adding to that the

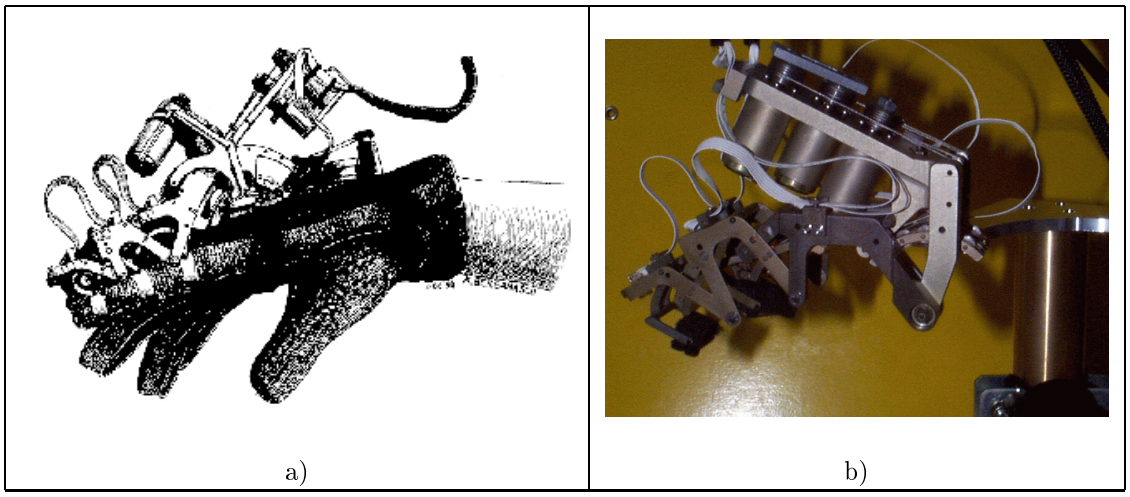

a) b)

**Figure 3.** (a) The HFF. (b) The TES

TES has only two points of attachment while the other three finger exoskeletons have three. Two force sensors, each of which obtained by 4 strain gauges, are located directly on dorsal surface of each phalange link. Rotation sensors, based on conductive plastic technologies, are integrated at each joint, recording the fingers' movements.

One of the critical factors encountered during the design of the system has been that of obtaining a system possessing limited weight and volumes, in such a way to allow good maneuverability of the hand. A solution has been found with the employment of a tension tendon drive system (fig.4). The three motors are located on a cantilever structure fixed with the base frame of each finger exoskeleton. The tendon drives for the distal and medial links (link 2 and 3) are unidirectional, meaning that they actuate only an extension movement. To maintain the tendon's tension in any operating condition two return springs are used. The proximal link (link 1) has instead a bi-directional tendon drive, while the base link is not actuated and its joint is passive, following the user's movements.

## 4. DYNAMIC MODEL FORMULATION

In the modelling of the TES it is useful to distinguish link 1, which has a bi-directional tendon drive, and links 2 and 3 for which the drive is unidirectional. The same model will be used for all the actuators being them all current controlled DC motors.

### 4.1. Actuators

Let us consider the case in which a power amplifier is used to control the current in the motor windings. The input command variable is the electromagnetic torque $\tau_{m,i}$ applied to the rotor. The dynamic model for the actuators takes as input also the load torque $\tau_{load,i}$ exerted by the driving pulley on the rotor and offers as output the motor angular position $q_{m,i}$. Note the presence of gearboxes on the motors' shafts whose reduction ratio is indicated by $N_i$. Indicating with $J_{m,i}$ and $b_{m,i}$, for $i = 1, 2, 3$, respectively the motor inertia and the viscous coefficient and with $\tau_{dp,i}$ and $J_{dp,i}$ respectively the torque applied by the transmission on the driving pulleys and the driving pulleys inertia, the actuator equations are:

$$\begin{aligned} J_{m,i}\,\ddot{q}_{m,i} + b_{m,i}\,\dot{q}_{m,i} &= \tau_{m,i} - \frac{\tau_{load,i}}{N_i} \\ J_{dp,i}\,\ddot{q}_{dp,i} &= \tau_{load,i} - \tau_{dp,i} \\ q_{dp,i} &= \frac{q_{m,i}}{N_i} \end{aligned}$$

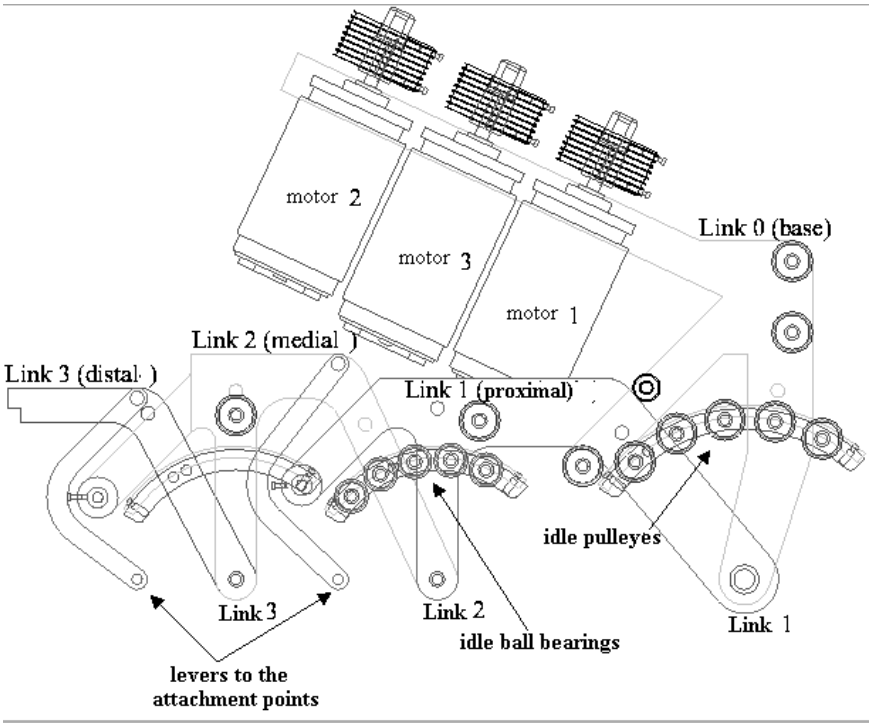


**Figure 4.** The TES structure.

from which we obtain the tranfer function

$$\frac{q_{m,i}}{\tau_{m,i} - \frac{\tau_{dp,i}}{N_i}} = \frac{1}{(J_{tot,i}\ s + b_{m,i})\ s} \tag{1}$$

where $J_{tot} = J_{m,i} + \frac{J_{dp,i}}{N_i^2}$.

### 4.2. Transmission

The transmission system interconnects the actuators with the links. The cables are modeled as a linear spring and a linear dashpot in parallel. This is an improvement with respect to considering the tendons ideally rigid; it allows to take into account at least the linear elastic effects and predict the frequencies and damping of the elastic resonant modes. The physical behavior of cables, especially those composed of many strands, is much more complex including non linear and hysteretic behaviors and delays in tension propagation. We will suppose the tension on a same tendon to be constant. This happens if the friction torque on the idle pulleys is negligible and the torque due to the pulleys inertia are small.

Referring to figure 5, indicating with $J_{l,i}$ the total inertia of link $i$ and its driven pulley, being $N_{t,i} := \frac{r_{ii}}{r_{dp,i}}$, $k_{t,i}$ and $b_{t,i}$ the transmission ratio, the elastic and viscous coefficient for tendon $i$, the following equations describing the dynamics of link 1 hold:

$$\begin{aligned} \tau_{m,1} = J_{m,1}\ \ddot{q}_{m,1} + b_{m,i}\dot{q}_{m,1} + \left[k'_t\ (q_{m,1} - q'_1) + b'_t\ (\dot{q}_{m,1} - \dot{q}'_1)\right] \\ J_1\ \ddot{q}'_1 = \left[k'_t\ (q_{m,1} - q'_1) + b'_t\ (\dot{q}_{m,1} - \dot{q}'_1)\right] = \frac{\tau_{dp,1}}{N_i} \end{aligned}$$

where $k'_t = \frac{2k_{t,1}r_{dp,1}^2}{N_i^2}$, $b'_t = \frac{2b_{t,1}r_{dp,1}^2}{N_i^2}$, $q'_1 = q_1\ N_i\ N_{t,1}$ and $J_1 = \frac{J_{l,1}}{(N_{t,i}N_i)^2}$. Using these equations it is easy to compute the block diagram representing the transmission for link 1 (fig. 6(a)). Such model is non linear due to some

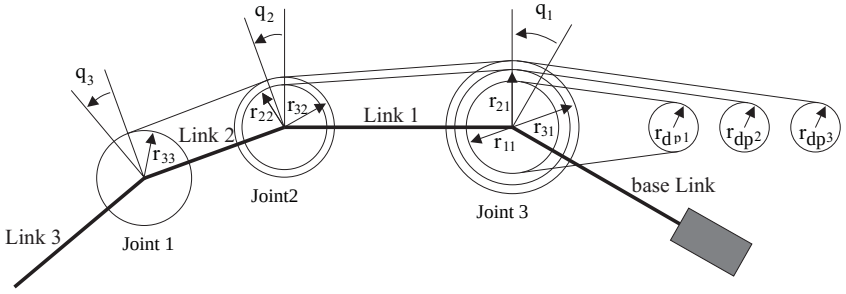


**Figure 5.** The TES transmission scheme.

effects as the engine friction and the joint friction, which have been described using a Reset Integrator Model,[3] and a gearbox model.

The equations that hold for links 2 and 3 are slightly different due to the unidirectionality. To describe such dynamics, which are strongly non linear, we will use function $u$ defined as

$$u(t) := \begin{cases} 0 & t < 0 \\ 1 & t \geq 0 \end{cases} \tag{2}$$

since the tendon's tension cannot be negative. The following equations hold[6]:

$$\begin{aligned} \tau_{m,1} - \frac{u(T_{t,i})\, T_{t,i}\, r_{dp,i}}{N_i} &= J_{m,i}\, \ddot{q}_{m,i} + b_{m,i}\dot{q}_{m,i} \\ \frac{\tau_{dp,1}}{N_i} &= \frac{u(T_{t,i})\, T_{t,i}\, r_{dp,i}}{N_i} \end{aligned}$$

where $T_{t,i}$ is the tension for tendon $i$. The block diagram for links 2 and 3 is presented in fig. 6(b).

It is important to express the coupling effect typical of tendon transmissions. Referring to fig.7 it appears clear that in static conditions the following holds:

$$\begin{aligned} q_{dp,1} &= -\frac{r_{11}}{r_{dp,1}}\, q_1 \\ q_{dp,2} &= -\Big(\frac{r_{21}}{r_{dp,2}}\, q_1 + \frac{r_{22}}{r_{dp,2}}\, q_2\Big) \\ q_{dp,3} &= -\Big(\frac{r_{31}}{r_{dp,3}}\, q_1 + \frac{r_{32}}{r_{dp,3}}\, q_2 + \frac{r_{33}}{r_{dp,3}}\, q_3\Big) \end{aligned}$$

and defined the $3 \times 3$ matrix $N$ as

$$N = \begin{bmatrix} N_1 \frac{r_{11}}{r_{dp,1}} & 0 & 0 \\ N_2 \frac{r_{21}}{r_{dp,2}} & N_2 \frac{r_{22}}{r_{dp,2}} & 0 \\ N_3 \frac{r_{31}}{r_{dp,3}} & N_3 \frac{r_{32}}{r_{dp,3}} & N_3 \frac{r_{33}}{r_{dp,3}} \end{bmatrix}$$

we have

$$\boldsymbol{q} = -\boldsymbol{N^{-1}}\, \boldsymbol{q_m}$$

Supposing that the transmissions don't imply any type of energy loss, matrix $N$ determines a linear relation between joint torque and motor torque given by

$$\boldsymbol{\tau_m} = -\boldsymbol{N^{-T}}\, \boldsymbol{\tau}$$

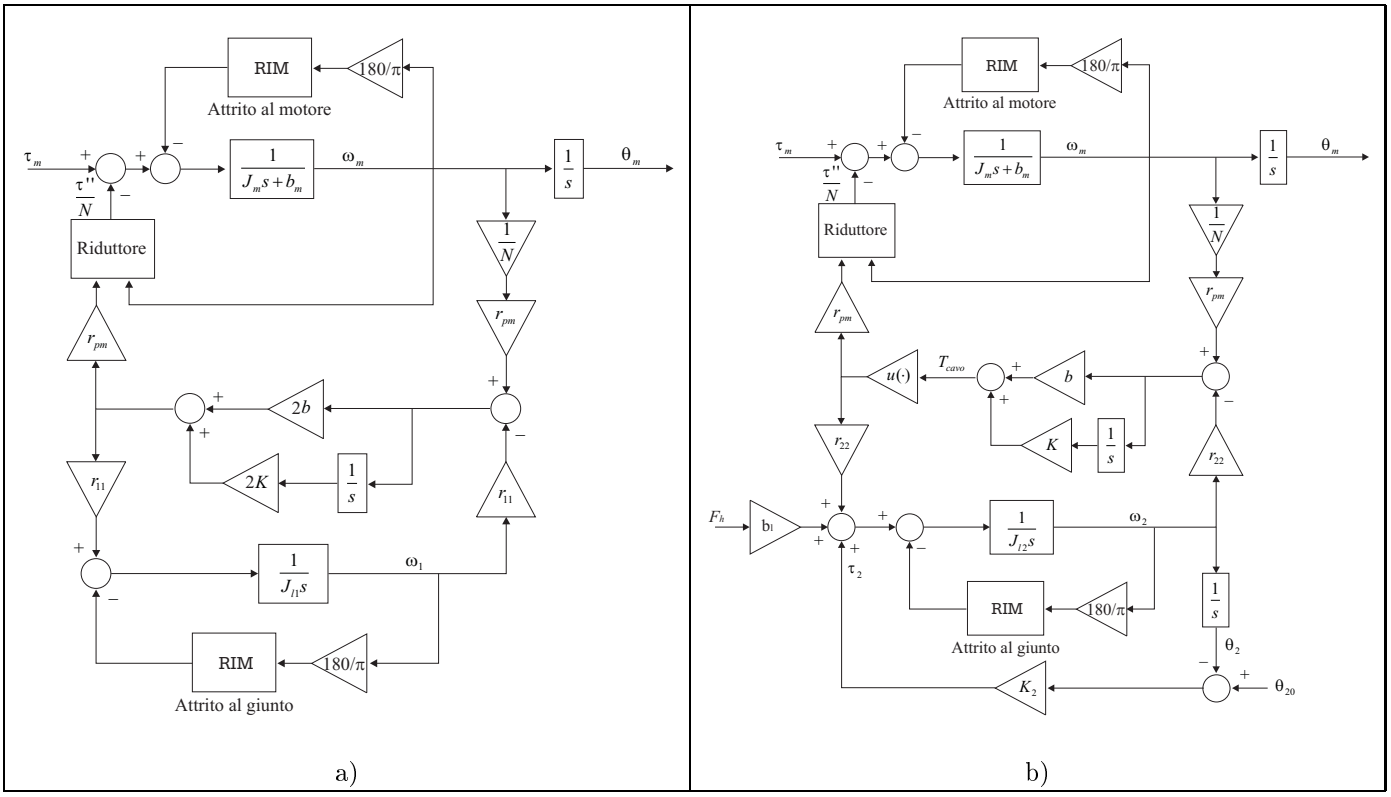


**Figure 6.** Nonlinear Model for (a) Link 1 and (b) Links 2/3.

### 4.3. Links

Referring to figure 7, if all inertial forces are neglected, considering the links to be ideally rigid and the system to be in equilibrium the following vectorial equation holds

$$\boldsymbol{\tau_m} = \boldsymbol{N^{-T}}\left(\boldsymbol{J^T(q)}\ \boldsymbol{f} + (\boldsymbol{\Phi} - \boldsymbol{K}\ \boldsymbol{q})\right) \tag{3}$$

being

$$\boldsymbol{K} = \begin{bmatrix} 0 & 0 & 0 \\ 0 & K_2 & 0 \\ 0 & 0 & K_3 \end{bmatrix} \boldsymbol{\Phi} = \begin{bmatrix} 0 \\ \Phi_2 \\ \Phi_3 \end{bmatrix}, \boldsymbol{J^T(q)} = \begin{bmatrix} 0 & b_2 + l_1 \cos q_2 & b_3 + l_2 \cos q_3 + l_1 \cos(q_2 + q_3) \\ 0 & b_2 & b_3 + l_2 \cos q_3 \\ 0 & 0 & b_3 \end{bmatrix}$$

the terms representing the return springs action on the links ($K_i$ :=elastic constant, $\Phi_i$ :=preload torque for return spring $i$) and $\boldsymbol{J^T(q)}\ \boldsymbol{f}$ the term representing the external forces action on the links. Note that element $\left(\boldsymbol{J^T(q)}\right)_{1,1}$ is null since the user can not apply any force to link 1 being no mechanical attachment to such part of the TES.

## 5. CONTROL DESIGN

The controller structure which has been adopted is shown in figure 8. External forces on links 2 and 3 are measured, compared to a reference desired force and processed by two separate control units (one for each link) independently. Considering equation (3) it is then easy to compute the desired motor torque. The compensation of the preload torque for transmissions 2 and 3 is obtained by the use of a proper unit. Finally matrix $\boldsymbol{N^{-T}}$ is used to get rid of the transmission coupling effect.

It is important to note that, due to the unidirectionality of transmissions 2 and 3, it is basic, for the TES to properly work, to impose torque for motors 2 and 3 to be always positive. Motor 1 on the other side is used only to

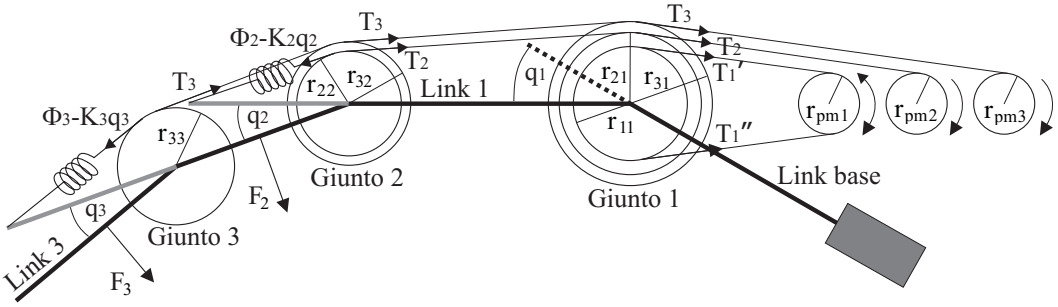


**Figure 7.** The TES transmission scheme in equilibrium.

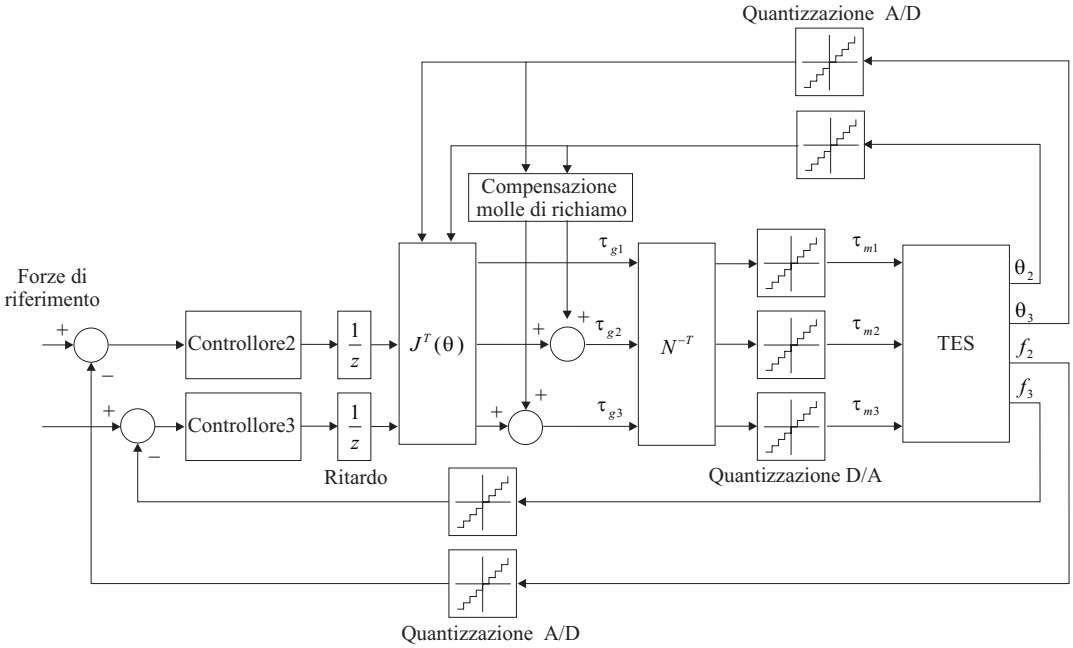


**Figure 8.** The TES control scheme.

get rid of the coupling effects proper to the tension tendon transmission. This might be problematic at times since the engines' limited power. Undesired side effects due to saturation appear to the user as unpredictable torque on link 1, which should be still and should follow the user's finger. In fact, by simply applying equation 3 to compute the motor torque there might be cases in which $\tau_{m,2}$ or $\tau_{m,3}$ won't be physically obtainable, saturating motor 2 or 3. In such case the algorithm commanding the TES should consider the real torque applied to links 2 and 3 to perfectly get rid of the coupling effect on link 1. Different algorithms have been used to approach this problem.

The digital control implementation has a sampling time of 0.5ms and introduces one cycle of delay for control law computing.

The purpose of the haptic control unit is to apply a desired force on the user's fingers. Desired forces are calculated by the virtual environment depending on if the user is interacting with any virtual object or not. The force servo which we implemented does not consider side effects such as gravity, dynamic coupling effects and friction. Two force controllers have been implemented. A proportional controller has been used to estimate the dominant poles of each link while a PID controller has been designed to obtain better performances. The latter controller is based on

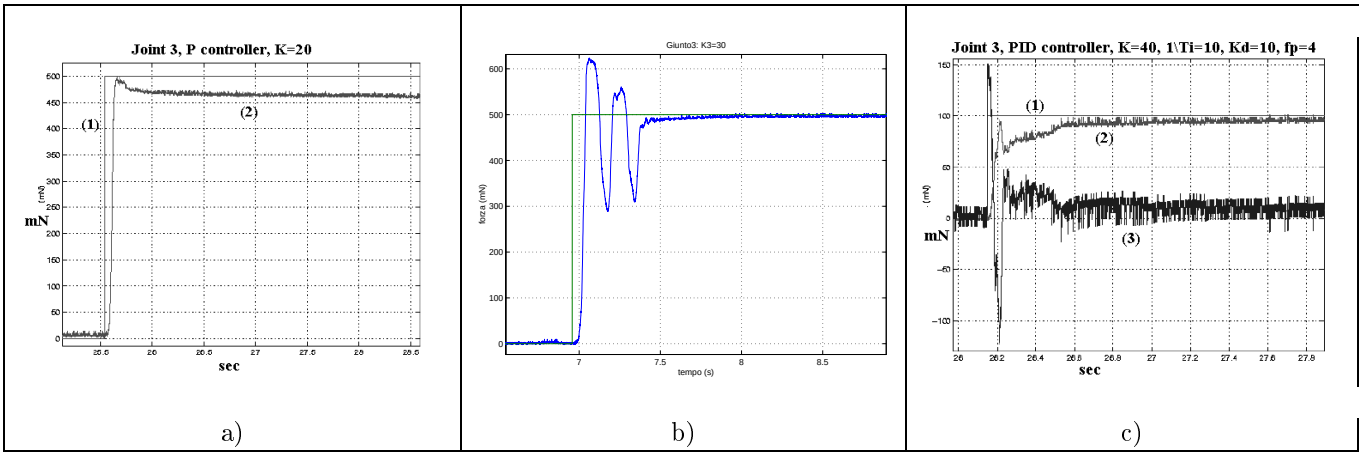


a) b) c)

**Figure 9.** Experimental results for Link 3 using: (a) a P controller with $K = 20$, (b) a P controller with $K = 30$, (c) a PID controller

three digital units, obtained by discretization of equation

$$f_c(t) = K(f_d(t) - f(t)) + \frac{1}{T_i}\int^t (f_d(x) - f(x))dx - K_d\frac{df(t)}{dt}$$

where $f(t)$ is the measured force, $f_c(t)$ is the control action applied to the TES and $f_d(t)$ is the desired action force. Practically, using a low-pass filter for the derivative block, we obtained the following discrete time functions

$$P(k) = K(f_d(k) - f(k)) \quad (4)$$

$$I(k) = I(k-1) + \frac{T}{T_i}(F_d(k-1) - F(k-1) \quad (5)$$

$$D(k) = \frac{T_d}{T+T_d}D(k-1) - \frac{K_d}{T+T_d}(f(k) - f(k-1)) \quad (6)$$

The Integral part has been realized with an anti wind-up mechanism trying to limit the actuators' saturation.

No simulations have been carried out yet on the TES model proposed in section 4 since some of the parameters could not be precisely estimated. This is one of the possible future developments of this work which will undoubtedly help designing more complex controllers with better overall performances.

When the user interacts with virtual objects the desired force is simulated to be elastic, being proportional to the angles at joints 2 and 3.

## 6. EXPERIMENTAL RESULTS

Two main types of experiments have been carried out: isometric experiments such as blocking link 2 or link 3 against an infinitely rigid environment, and functional tests such as having a user wear the interface making free movements (isotonic conditions) or interacting with a deformable virtual object.

The isometric experiments have been carried out on the TES blocking link 2 (or link 3) and applying to motor 2 (or 3) a step input force of varying in a range between 100mN and 500mN. The result of such experiments, using a Proportional and a PD and a PID controller, are hereafter presented.

First of all let's focus our attention on the experiments carried out on link 3. Referring to fig.9, function (1) is the step input force to be followed, function (2) is the measured force, function (3) (in fig. c) is the control signal. Experiment (a) has been conducted using a P controller with $K = 20$ while experiment (b) using $K = 30$. In both cases the step input to be tracked has a 500mN magnitude. Increasing gain $K$ further we obtain more oscillating

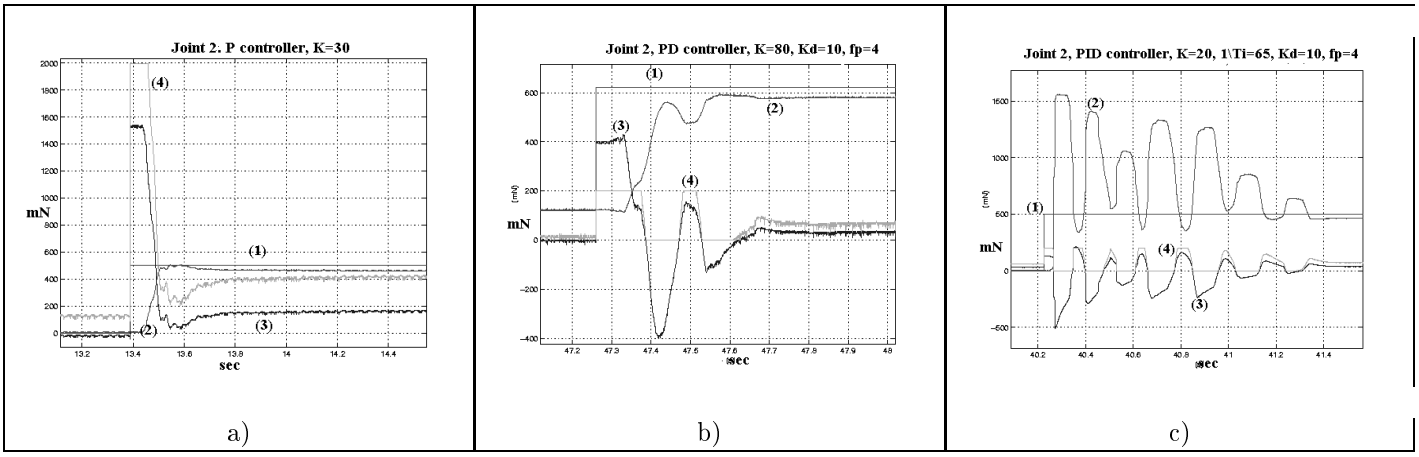


a) b) c)

**Figure 10.** Experimental results for Link 2 using: (a) a P controller with $K = 30$, (b) a PD controller, (c) a PID controller

signals until the system becomes unstable for gains $K > 50$. Experiment (c) is referred to a PID controller with $K_p = 140$, $\frac{1}{T_i} = 10$, $K_d = 10$ with a low-pass filter on the measured force signal. Such filter has a pole at 4Hz and a gain equal to 10. The step input to be tracked has a intensity of 100mN. Both the rise time, the overshoot, the settling time are better using the latter controller giving overall better performances. The position-error is null in the latter case due to the integral block of the controller.

Secondly, let's focus on the experiments carried out on link 2. Signals (1)-(4) have the same meanings as the ones indicated above. Considering fig.9, function (1) is the step input force to be tracked, function (2) is the measured force, function (3) is the control signal while function (4) is the control signal practically obtained on the motors. Experiment (a) is referred to a Proportional controller with $K = 30$, experiment (b) is referred to a PD controller with $K_p = 80$ and $K_d = 10$ and experiment (c) is referred to a PID controller with $K_p = 20$, $K_d = 10$ and $\frac{1}{T_i} = 65$. All experiments have been conducted tracking a force step input having a 500mN intensity.

In all of these experiments the system always responds with a finite time delay. This is due to a not prefect blocking system for link 2. Experiment (a) has the best performance overall even though the motors saturate. Increasing the proportional gain we obtain a prompter response an a higher overshoot until reaching $K > 70$, which is the threshold when the system becomes unstable. The PD controller (fig.10,b) has better response and overshoot performances but these are not so far from the simpler P controller. Motors tend to saturate even more and the control action is highly non-linear. The PID controller has a better position-error, even though it's not null due to frictions of the gearbox. The overshoot though is definitely too high probably due to the delays on the motor's action introduced by a friction of the gearboxes.

Let us now consider the functional experiments on link 3. Such a controller has been realized to simulate a soft deformable object with elastic constant $k = 50$mN per joint angle degree. Experiments conducted on link3 are presented in fig.11 and in fig.12. More specifically fig.11a represents joint angle $q_3$ and fig.11b represents the measured force obtained on link 3 when the deformable object is implemented, while fig.12a represents joint angle $q_3$ and fig.12b represents the measured force obtained on link 3 when the deformable object is not implemented. Figure 11 shows clearly how the measured force is proportional to the angle at joint 3 while figure 12 shows how, being the contact with the deformable elastic object not simulated the measured force is independent from the angle at joint 3 and the force disturbance is not higher than 0.2mN.

## 7. CONCLUSIONS

This paper presents for the first time some experiments carried on the HFF haptic interface designed at PERCRO lab. A haptic servo force controller has been designed and tested for such system. The control of link 2 appears to be harder than the one of link 3. This is due to the higher friction of motor 2 gearbox. The tension tendon transmission is one of the key issues to be solved when designing a controller for the TES. Such a type of drive implies a coupling

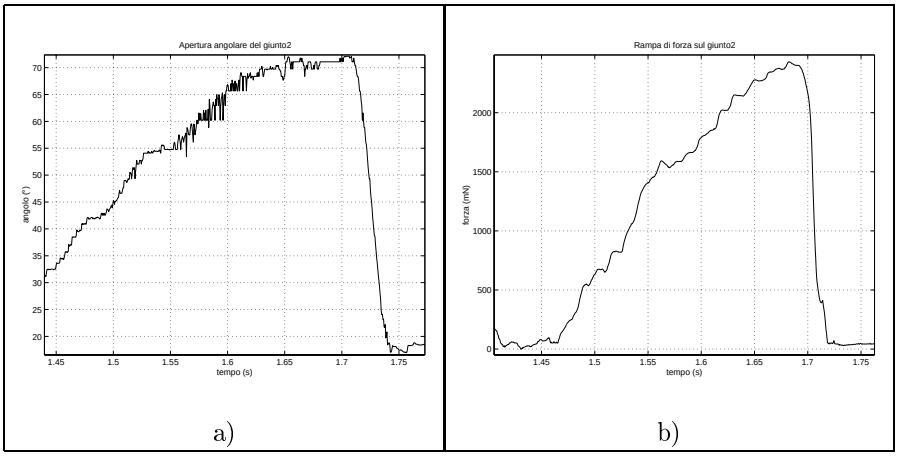


**Figure 11.** Experimental results interacting with a virtual elastic object: (a) joint angle 3, (b) measured force on link 3

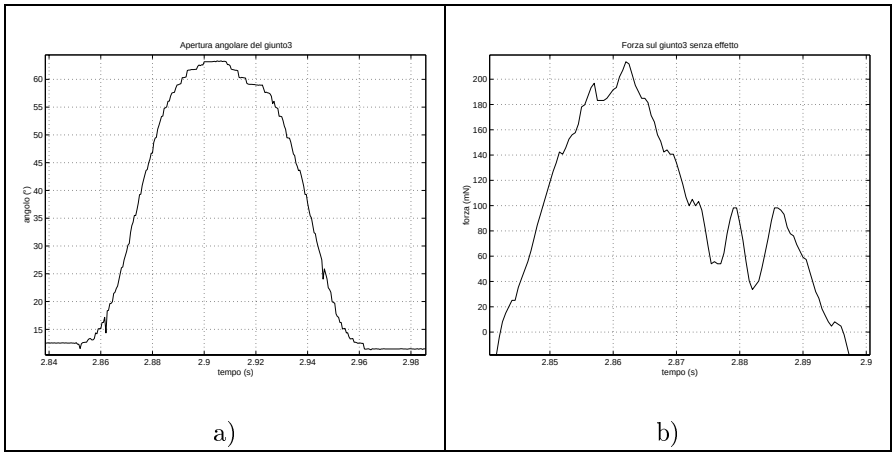


**Figure 12.** Experimental results without a virtual elastic object: (a) joint angle 3, (b) measured force on link 3

effect between different links which is made worse by the fact that motors tend to easily saturate. Moreover the nonlinear model which has been presented, which is highly innovative, has not been used for simulations yet due to the lack of precise estimates for some of the system's parameters. The unidirectionality of two of the drives makes the controller design more complex. One possible solution, proposed in the article, is keeping a minimum tension in the transmission by constraining the motor's minimum torque. However a new mechanical project using three bi-directional drives will be soon presented.

## REFERENCES

1. Bergamasco M., "Force Replication to the Human Operator: the Development of Arm and Hand Exoskeletons as Haptic Interfaces",*ISRR*, Munich, 1995
2. Burdea G., "Force and Touch Feedback for Virtual Reality", *Wiley*, New York, 1996
3. Haessig D. A., Frieland B., "On the modelling and simulation of friction", *J. of dynamic systems, measurements and control* September 1991
4. Hayward V., Cruz-Hernandez J. M., "Parameter Sensitivity Analysis for Design and Control of Tendon Transmissions", *ISER*, Stanford, 1995

5. Jacobsen S. C., Ko. H, Iversen E. K., Davis C. C., "Antagonistic Control of a Tendon Driven Manipulator", *ICRA*, Scottsdale, 1989
6. Prisco G. M., Bergamasco M., "Dynamic Modelling of a Class of Tendon Driven Manipulators", *ICAR*, Monterey, 1997
7. Prisco G. M., Bergamasco M., "Preliminary Considerations on the Design of Controllers for Haptic Interfaces", *SPIE*, Philadelphia, 1997
8. Townsend W. T., "The Effect of Transmission Design On The Performance of Force-controlled Manipulators", PHD thesis, MIT,1988